V. Bruschi, V. Välimäki, J. Liski and S. Cecchi,
"Linear-Phase Octave Graphic Equalizer"
J. Audio Eng. Soc., vol. 70, no. 6, pp. 435–445, (2022 June).
DOI: https://doi.org/10.17743/jaes.2022.0014

Linear-Phase Octave Graphic Equalizer

VALERIA BRUSCHI,[1,2]* *AES Student Member*, **VESA VÄLIMÄKI,**[1] *AES Fellow*,
(v.bruschi@staff.univpm.it) (vesa.valimaki@aalto.fi)
JUHO LISKI,[1] **AND STEFANIA CECCHI,**[2] *AES Associate Member*
(juho.liski@aalto.fi) (s.cecchi@staff.univpm.it)

[1] *Acoustics Lab, Department of Signal Processing and Acoustics, Aalto University, FI-02150 Espoo, Finland*
[2] *Department of Information Engineering, Universitá Politecnica delle Marche, 60124 Ancona, Italy*

A computationally efficient octave-band graphic equalizer having a linear-phase response is introduced. The linear-phase graphic equalizer is useful in audio applications in which phase distortion is not tolerated, such as in multichannel equalization, parallel processing, phase compatibility of audio equipment, and crossover network design. The structure is based on the interpolated finite impulse response (IFIR) philosophy. The proposed octave-band graphic equalizer uses one prototype low-pass filter, which is a half-band FIR filter designed using the window method. Stretched versions of the prototype filter and its complementary high-pass filter implement all ten band filters needed. The graphic equalizer is realized in the parallel form, in which the outputs of all band filters, scaled with their individual command gain, are added to compute the equalized output signal. The command gains can be used directly as filter band gains. The number of operations needed per sample is only slightly more than that needed for the graphic equalizer based on minimum-phase recursive filters. A comparison with other implementation approaches demonstrates that the proposed structure requires 99% fewer operations than a high-order FIR filter. The proposed filter uses 39% fewer operations per sample than the fast Fourier transform–based filtering method and causes over 78% less latency.

0 INTRODUCTION

Graphic equalizers (GEQs), named after the fact that the user controls plot the approximate magnitude response [1–3], are widely used in audio. The bands of the GEQ have a fixed center frequency and a fixed bandwidth, so the user can adjust only the gain of each band by changing slider positions. This paper focuses on the design of a computationally efficient linear-phase GEQ composed of finite impulse response (FIR) band filters.

Analog GEQs have minimum phase, which is a widely used property for digital GEQs as well. Minimum-phase EQs have, by definition, the smallest possible latency making them highly suitable for live music applications, for example. In addition, they do not produce pre-ringing artifacts, because the impulse response of the EQ is zero before the main spike. However, for certain applications, such as multichannel equalization, parallel processing, phase compatibility of audio equipment, and crossover network design, minimum-phase EQs are undesirable.

For example, in multichannel audio equalization, in which the target magnitude responses for different channels vary, the phase responses differ as a result, which can affect the spatial impression [4]. A linear-phase GEQ is thus required for these applications, because it retains the original phase of the signal [5] and does not produce phase distortions that might cause undesired audible effects, especially equalizing speech [6].

Traditionally, a GEQ is formed by a set of infinite impulse response (IIR) filters connected either in cascade [7, 1, 8, 9] or parallel [1, 10–12], and only the band filter gains are adjustable [13]. Recently, good accuracy has been reached using band filters that are second-order IIR sections (also known as biquads), which results in a low overall filter order and a small number of operations per sample [14, 9, 12].

With an IIR-based GEQ, the phase response is typically minimum phase, even though other phase responses are also possible. The other phase responses often require high filter orders or the phase response is only an approximation [15], so they are not considered further. On the other hand, when a linear-phase response is desired, FIR filters may be used [3], because they can have an arbitrary phase response. An

* To whom correspondence should be addressed, e-mail: v.bruschi@staff.univpm.it. Last updated: Mar. 30, 2022

additional advantage of FIR filters is that they do not suffer from numerical problems, which may require attention in IIR filter implementations [16]. Digital FIR GEQs have existed since the 1980s [17–19], and similarly to IIR GEQs, the parallel structure is an option [17, 18, 20].

An FIR GEQ can also be implemented as a single high-order filter [20]. The single FIR filter is used to approximate the target frequency response specified by the user [20]. This can be based on the interpolation of the target curve [19, 21], which is not a trivial task, because the EQ target curve is not well-defined between the command-gain points. In addition, the filter length is determined by the lowest band filter, and in order to accurately match the target response at low frequencies, a filter order of at least several thousand is required [19, 22–24]. Moreover, depending on the design, the single FIR may need to be redesigned completely whenever a gain is modified, requiring additional computing, which is unsuited for real-time modifications of the target response.

There are ways to affect the computational cost of FIR GEQs. Frequency-warped FIR filters [25, 26] can be used to shorten the required filter lengths, especially at low frequencies. This, however, results in a nonlinear-phase response, because of the warped FIR filters being IIR filters in practice. This is why frequency warping is not considered further here.

Fast convolution [27] is also used in FIR GEQ design to reduce the computational cost [28–31]. Here, the equalization is achieved as the complex multiplication of the discrete Fourier transforms of the signal and the filter's impulse response, inverse transforming the result, and processing the signal this way in frames. The transformations are realized using the fast Fourier transform (FFT), which ensures computational efficiency. The frame-based processing causes much latency, but the FFT-based processing allows for a linear-phase response [29].

Multirate processing can be applied to implement a linear-phase FIR GEQ [18, 19, 32, 23]. In multirate GEQs, the sample rate may differ for all band filters so that the highest frequency band uses the largest sample rate, whereas the lowest frequency band uses the slowest rate. After the filtering, all bands are upsampled back to the original sample rate and are summed.

Hergum [33] proposed an interesting FIR GEQ design, which is based on interpolated FIR (IFIR) filters [34]. Recently, a similar design was proposed for another band division [35]. An IFIR filter contains a cascade of two filters with the first producing a periodic frequency response and the second attenuating the unwanted repetitions [34]. IFIR filters achieve linear-phase and small ripple at a low computational cost. Although Hergum's design is clever and efficient, the audio frequencies are divided in equal bands, as is the case with the equalizer proposed in [35]. This is incompatible with standard graphic equalizers, which use a logarithmic band division [3].

This paper proposes an efficient linear-phase GEQ based on IFIR filters. The design utilizes an octave band division, and its band filters are arranged in a parallel structure. In this way, the design has logarithmically spaced center frequencies, which is mandatory in audio applications because of the human perception of sound and the nature of music. The accuracy of the proposed design is comparable with the state-of-the-art IIR GEQs having an approximation error less than ± 1 dB at the center frequencies. The linear-phase characteristic is achieved with a minor increase in computational cost compared with the IIR filter-based designs. In comparison with previous linear-phase FIR GEQ designs, the proposed design achieves a similar accuracy with a reduced latency and an improved computational efficiency.

The structure of the paper is as follows. SEC. 1 describes in detail the structure and the design of the proposed linear-phase GEQ based on IFIR filters and shows the performance of the proposed system. SEC. 2 compares the proposed and other linear-phase FIR GEQ designs. Finally, the conclusions are presented in SEC. 3.

1 PROPOSED GRAPHIC EQUALIZER DESIGN

This section proposes the new design for a linear-phase GEQ in parallel form. The octave equalizer is considered with the following ten band center frequencies, or command frequencies: 31.25 Hz, 62.5 Hz, 125 Hz, 250 Hz, 500 Hz, 1.0 kHz, 2.0 kHz, 4.0 kHz, 8.0 kHz, and 16.0 kHz. The bands are numbered from lowest to highest using index $m = 1, 2, 3, ..., 10$. This design uses the sample rate of $f_s = 48$ kHz, which is common in professional and mobile audio.

1.1 Filter Structure

The overall scheme of the proposed linear-phase octave-band equalizer is shown in Fig. 1. The proposed structure is a tree structure similar to the scheme obtained by classic wavelet transformation [36]. The highest band is obtained by the signal path at the top of the figure and the lowest one by the path at the bottom. The final output is computed by summing the branch outputs.

The filterbank of Fig. 1 is designed starting from a half-band low-pass prototype FIR filter $H_{\mathrm{LP}}(z)$, which must be symmetric and of odd length, i.e., even order. The delay D to the center point of the prototype filter, in samples, is $D = N/2$, where N is the prototype filter order, which is even. Thus, the filter length, which is $N + 1$, is odd, and the delay D is an integer.

The highest band of the equalizer $H_{10}(z)$ is designed as a complementary high-pass filter $H_{\mathrm{HP}}(z)$ of the prototype filter, so $H_{10}(z) = H_{\mathrm{HP}}(z)$, as follows:

$$H_{\mathrm{HP}}(z) = z^{-D} - H_{\mathrm{LP}}(z). \tag{1}$$

Because of the fact that integer interpolation factors are used, the cutoff frequency of the low-pass filter is $f_c = 12$ kHz, which is half of the Nyquist limit of 24 kHz. In the proposed design, this corresponds to the cutoff frequency of the highest band, which, in an octave GEQ, is the band edge between the 8-kHz and 16-kHz octave bands equaling to $\sqrt{8 \times 16} \approx 11.3$ kHz. Therefore, the cutoff frequency of the proposed highest band filter is slightly shifted with respect to the usual octave-band filterbank. This does not

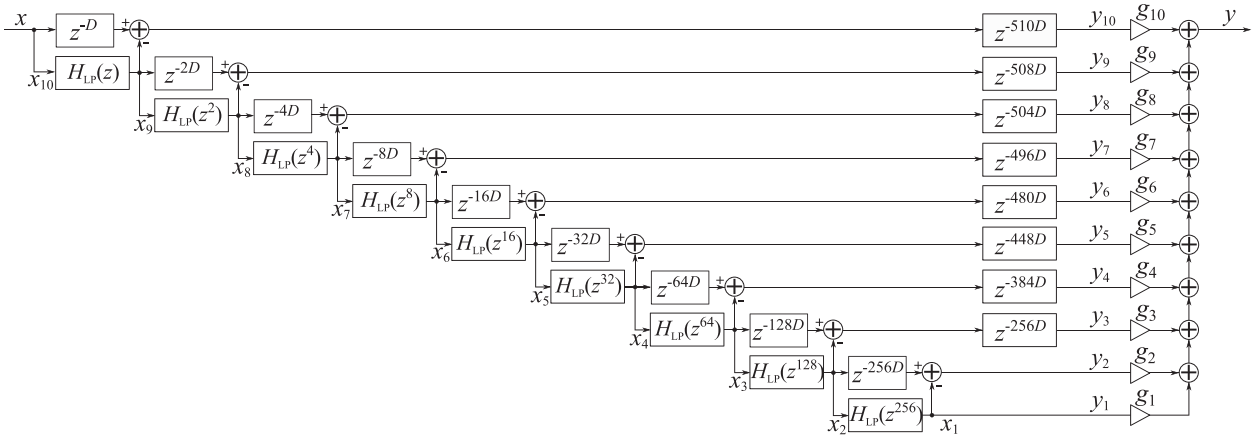

Fig. 1. Block diagram of the proposed parallel graphic equalizer for ten octave bands. The signal path at the top produces the highest band (16 kHz), whereas the bottom one produces the lowest band (31.25 Hz).

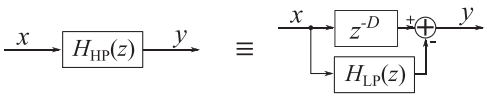

Fig. 2. Scheme of the complementary filter.

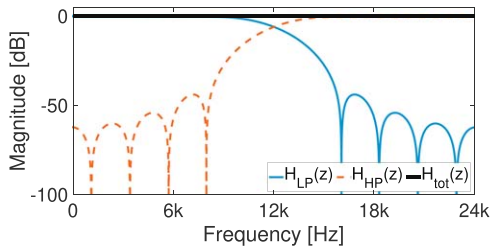

Fig. 3. Magnitude response of the prototype low-pass filter, its complementary high-pass filter, and the total response of their sum.

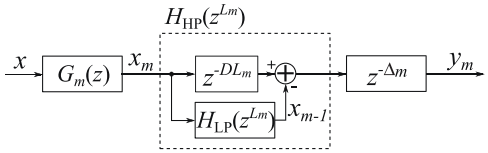

Fig. 4. Filters and delay lines associated with a single band for $m = 2, 3, ..., M$, cf. Fig. 1. This mth band transfer function $H_m(z)$ represents the relation between $Y_m(z)$ and $X(z)$.

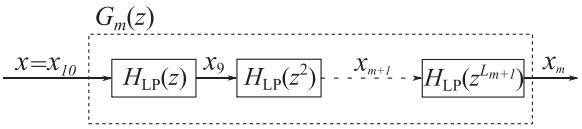

Fig. 5. Details of the transfer function $G_m(z)$ used in Fig. 4.

affect the final realization or accuracy of the graphic equalizer, as it is only required to monitor the magnitude error at the command frequencies.

According to Eq. (1), the filter $H_{\mathrm{HP}}(z)$ can be implemented using a delay line and a subtraction once the lowpass filtered signal going to the lower bands has been computed using $H_{\mathrm{LP}}(z)$, as shown in Fig. 2. In addition to computational efficiency, another advantage of complementary filters is the fact that the total response is completely flat, when the neighboring band filters have the same gain, as shown in Fig. 3. Hergum also pointed out this advantage in his study [33].

The rest of the bands of the filterbank are obtained with stretched versions of the prototype filter, such as $H_{\mathrm{LP}}(z^2)$ and $H_{\mathrm{LP}}(z^4)$, which are prepared by inserting one or three zero samples between each two coefficients of the prototype FIR filter, respectively [37]. The general scheme of delay and filtering operations for the mth band is presented in Fig. 4. The Z transform of the mth band output signal $Y_m(z)$ is obtained from the input signal $X(z)$ as follows:

$$Y_m(z) = H_m(z)X(z), \tag{2}$$

where $H_m(z)$ is the transfer function of the mth band and is computed as

$$H_m(z) = z^{-\Delta_m}[z^{-DL_m} - H_{\mathrm{LP}}(z^{L_m})]G_m(z), \tag{3}$$

where the mth interpolation factor L_m is computed as

$$L_m = 2^{(M-m)} = 2^{(10-m)}, \tag{4}$$

and the transfer function $G_m(z)$, which is shown in detail in Fig. 5, is composed of the cascade of all previous band filters:

$$G_m(z) = H_{\mathrm{LP}}(z) \prod_{k=m+1}^{M-1} H_{\mathrm{LP}}(z^{L_k}), \tag{5}$$

with $m = 2, 3, ..., M$ and $M = 10$. Looking at Fig. 4, the input signal $x(n)$ is first filtered by the filter $G_m(z)$, and the resulting intermediate signal $x_m(n)$, shown for each band in Fig. 1, is then filtered by $H_{\mathrm{HP}}(z^{L_m})$ that is implemented through a delay line and a subtraction, according to Eq. (1). Note that in Fig. 4, when $m = 9$, the signal $x_{10}(n)$ corresponds to the input signal $x(n)$, which is also seen in the top left corner in Fig. 1.

Fig. 6 shows a design example of the sixth band, with a center frequency of 1 kHz. In this case, the transfer function

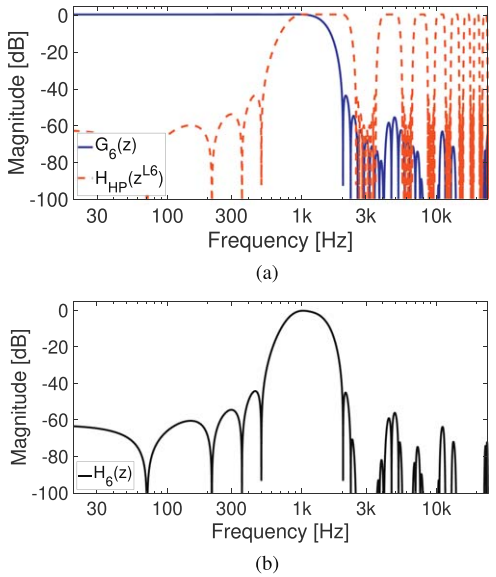

Fig. 6. Example of the design of the magnitude response of the band filter centered at 1 kHz. Cascading the filters (a) $G_6(z)$ and $H_{\mathrm{HP}}(z^{L_6}) = z^{-DL_6} - H_{\mathrm{LP}}(z^{L_6})$ results in (b) the band filter $H_6(z)$.

of the sixth band $H_6(z)$ is obtained by the concatenation of the filter $G_6(z)$ and the filter $H_{\mathrm{HP}}(z^{L_6}) = z^{-DL_6} - H_{\mathrm{LP}}(z^{L_6})$.

A synchronization delay Δ_m, also shown in Fig. 4, must be applied in order to align all the band outputs and is determined as follows:

$$\Delta_m = \tau - [2^{(M+1-m)} - 1]D = \tau - [2^{(11-m)} - 1]D, \quad (6)$$

where τ is the total delay of the equalizer in samples:

$$\tau = [2^{(M-1)} - 1]D = 511D. \quad (7)$$

In Fig. 1, the synchronization delays Δ_m are shown one upon the other on the right-hand side, next to the command gain factors g_m. In the highest band (the top signal path in Fig. 1), the total delay of $511D$ samples is formed by the cascade of the delay line z^{-D} and the synchronization delay z^{-510D}. In the lowest band, the synchronization delay is formed by the cascade of all the delay lines between the input (top left corner in Fig. 1) and the output y_1 (bottom right corner in Fig. 1), which have the lengths D, $2D$, $4D$, $8D$, $16D$, $32D$, $64D$, $128D$, and $256D$. This adds up to $511D$ samples of delay.

The lowest band filter of the equalizer is obtained as a byproduct, when the signal $x_2(n)$ is filtered with the prototype filter stretched by a factor of 2^8, or 256, as shown in Fig. 1. The resulting signal $x_1(n)$ does not require further processing, as it is the output signal $y_1(n)$ of the lowest band filter. The filter $H_{\mathrm{LP}}(z^{256})$ also implements the largest input–output delay, so a synchronization delay is unnecessary in the two lowest bands, as seen in Fig. 1.

Finally, as presented in Fig. 1, the desired gain factor g_m of each band is applied, and the total response of the equalizer $y(n)$ is obtained as a weighted sum of all band output signals:

$$y(n) = \sum_{m=1}^{M} g_m y_m(n). \quad (8)$$

Since the band filters determine the gain on their own band very accurately, optimization of filter gains is unnecessary, and command gains can directly be used as weights g_m. This is an advantage with respect to recursive GEQs, for those applications in which command gains are varying constantly, such as unmasking EQs for ambient noise [38].

1.2 Prototype Filter Design

The overall performance of the proposed GEQ depends on the prototype filter $H_{\mathrm{LP}}(z)$, which is imposed to be a half-band low-pass filter. A peculiarity of half-band filters is the fact that one every two samples of the impulse response is zero by definition, except for the middle coefficient [37]. This characteristic allows one to reduce the computational cost by avoiding multiplications with zero coefficients during the filtering computation. Moreover, the linear-phase characteristic implies that the impulse responses are symmetric, approximately halving the number of multiplications.

The FIR filter could be designed by optimization methods, as the least squares or the Remez algorithm [39], or by other efficient possibilities, such as a method based on iterated sine [40]. In contrast, in this paper, the filter is designed using the windowing technique [39], which is the simplest method, but effective for the proposed system. Starting from the cutoff frequency $f_c = 12$ kHz, the prototype filter coefficients are computed as follows:

$$h_{\mathrm{LP}}(n) = w(n)\left[\frac{\sin\left(\omega_c(n - D_{\mathrm{win}})\right)}{\pi(n - D_{\mathrm{win}})}\right], \quad (9)$$

where $\omega_c = 2\pi f_c/f_s$, $w(n)$ is the window function applied, and D_{win} is the delay of the filter. Assuming L_{win} as the length of the filter, which is obtained as $L_{\mathrm{win}} = N + 1$, with N the filter order, the delay D_{win} is calculated as $D_{\mathrm{win}} = (L_{\mathrm{win}} - 1)/2 = N/2$.

In this study, several window functions $w(n)$ have been tested for the design of the prototype filter: rectangular, Bartlett, Hamming, Hanning, Blackman, and Kaiser window. The rectangular and the Bartlett (triangular) windows are characterized by a modest attenuation in the stopband. For this reason, they do not guarantee an acceptable performance and have not been included in the paper. The Hamming and Hanning windows have similar properties in terms of transition band and attenuation. The Blackman method ensures the largest stopband attenuation but has a wide transition band. The attenuation of the Kaiser window depends on the parameter β: a bigger β guarantees a higher attenuation in the stopband of the filter [41]. In view of this, only Hamming, Hanning, Blackman, and Kaiser methods are considered in the following. Fig. 7 and Table 1 show an example filter design, using the Kaiser window with a

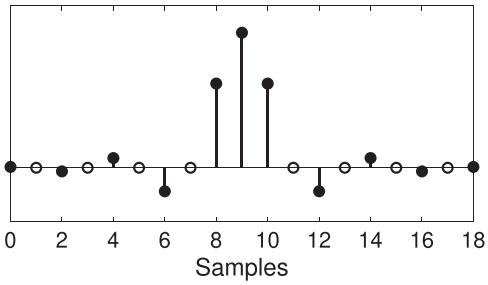

Fig. 7. Design of the prototype filter with the Kaiser window ($\beta = 4$). The filter length is $L_{win} = 19$, but it has only $N_{nz} = 11$ nonzero coefficients (shown with black dots).

Table 1. Coefficients of the FIR prototype filter of Fig. 7.

Index	Value	Index	Value
0	0.00313	10	0.31158
1	0	11	0
2	–0.01338	12	–0.08718
3	0	13	0
4	0.03593	14	0.03593
5	0	15	0
6	–0.08718	16	–0.01338
7	0	17	0
8	0.31158	18	0.00313
9	0.5		

length of $L_{win} = 19$ and $\beta = 4$. The final filter has an order of $N = 18$ and the number of nonzero elements is $N_{nz} = 11$.

1.3 Performance of the Proposed Equalizer

The proposed equalizer is evaluated in terms of error of the magnitude response, comparing different orders and four windowing methods for the prototype filter design: Hamming, Hanning, Blackman, and Kaiser. The latency and the computational complexity are proportional to the filter order. For the experiments, a sampling frequency of 48 kHz was used. For the Kaiser window, the parameter value $\beta = 4$ is chosen for all the simulations after empirical studies, because it ensures the lowest error when using low filter orders, i.e., when having as low computational cost as possible. Lower values of β do not guarantee a sufficient attenuation to obtain an acceptable accuracy. Instead, higher values allow to obtain a better attenuation, but the error of the total equalizer becomes acceptable only by increasing the filter order.

Table 2 shows the obtained results. The error is calculated as the maximum difference between the desired and the obtained gains at the octave center frequencies, considering all the possible configurations with ± 12 dB, which leads to 1,024 cases in total [42]. Moreover, when two adjacent bands have the same gain, the error is computed as the maximum deviation from the straight line that connects the two gains at the center frequencies. The error is considered acceptable when it is below 1 dB, according to previous publications that applied the same method to have a quantitative estimation of the GEQ accuracy [43, 42]. In addition, in [44, 45], listening experiments have proven that the audible peak level for octave filters is below 1 dB when white noise is considered as input, whereas the just noticeable difference in the deviation of the magnitude response is higher than ± 1 dB with other signals, as declared also in [46].

In Table 2, $L_{win} = 19$ is the lowest filter length considered, because it is the shortest window that leads to a 1-dB accuracy, and all shorter windows tested lead to a larger error. Looking at Table 2, it is worth noting that sometimes the error increases with the increase of the filter order. In particular, this happens with Kaiser and Hanning windows that are characterized by a lower attenuation. In fact, the increase of the filter order N makes the transition band steeper but produces more lobes in stopband maintaining the same attenuation, as shown in Fig. 8. These lobes can cause a wider ripple on the total response of the GEQ that may make the error exceed 1 dB, especially when the command gain is -12 dB. The latency τ is the delay in samples of the total equalizer and is computed following Eq. (7).

The filtering is implemented avoiding the operations with zero elements of the filter, so the number of multiplications for each output sample is calculated as follows:

$$\text{n}^\circ \text{ mult.} = (M - 1)N_{nz} + M, \tag{10}$$

Table 2. Performance of the proposed equalizer with varying lengths and designs of the prototype low-pass filter. The error is calculated as the largest maximum difference between the desired and the obtained gains, considering all the possible configurations with ± 12 dB (1,024 test cases). The designs having their maximum error below 1 dB are highlighted by the bold text.

L_{win}	N (N_{nz})	τ	Mul (sym)	Add	Window	Err [dB]
19	18 (11)	4,599	109 (64)	108	**Kaiser**	**0.79**
					Hamming	2.44
					Hanning	**0.99**
					Blackman	5.92
27	26 (15)	6,643	145 (82)	144	Kaiser	1.03
					Hamming	1.99
					Hanning	1.13
					Blackman	**0.76**
55	54 (29)	13,797	271 (145)	270	**Kaiser**	**0.82**
					Hamming	**0.96**
					Hanning	**0.91**
					Blackman	**0.05**

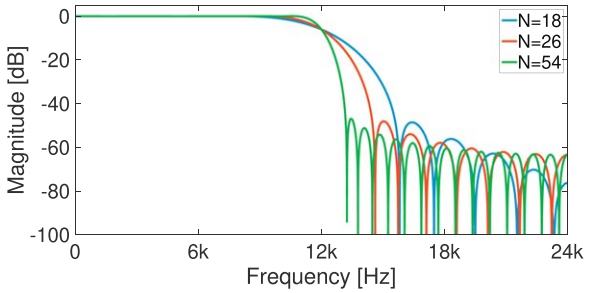

Fig. 8. Design of the prototype lowpass filter varying the order N, using a Kaiser window function with $\beta = 4$.

where N_{nz} is the number of nonzero elements of the prototype filter, and $M = 10$ is the number of bands. The number of multiplications can be further reduced by accounting for the symmetry of the impulse responses as follows:

$$\text{n}^\circ \text{ mult. (sym)} = (M-1)\frac{N_{\text{nz}}+1}{2} + M. \tag{11}$$

Finally, the number of additions is computed as follows:

$$\text{n}^\circ \text{ add.} = (M-1)N_{\text{nz}} + M - 1. \tag{12}$$

Analyzing the results of Table 2, the Blackman technique with $L_{\text{win}} = 57$ shows the lowest error (0.05 dB), but the computational cost (541 operations per sample) and the latency (13,797 samples, or 287 ms) are the highest. A latency that large is unacceptable for some applications, such as live sound or sound with moving image; however, for audio playback, without visual or other reference, even such a latency may be acceptable. The Hamming window has the worst performance in terms of both computational cost and error. Finally, the Hanning method with $L_{\text{win}} = 21$ and the Kaiser method with $L_{\text{win}} = 19$ both guarantee an acceptable error (below 1 dB) with the lowest computational cost (64 multiplications and 108 additions, or 172 operations per output sample). The Kaiser technique shows a lower error equal to 0.79 dB, is thus considered the best design, and is used in the comparison with the other methods. The total latency of the equalizer is $\tau = 4{,}599$ samples, or 95.8 ms at the sample rate of 48 kHz.

The output signals of each band of the proposed equalizer as a response to a unit impulse are shown in Fig. 9 from the highest band (on the top of the figure) to the lowest one (on the bottom). All band filters are seen to be symmetric, which implies a linear-phase response.

Fig. 10 shows the magnitude frequency response of each band and the total frequency response of the equalizer when all the gains are set to the same value of 0 dB. The use of complementary filters guarantees a completely flat total response. Even if the single bands present ripple, the total response is flat thanks to the compensation of the stopband ripples of the adjacent filters, as shown in Fig. 10(b).

Fig. 11 shows example magnitude frequency responses of three different test configurations:

(a) the zigzag command settings (±12 dB);

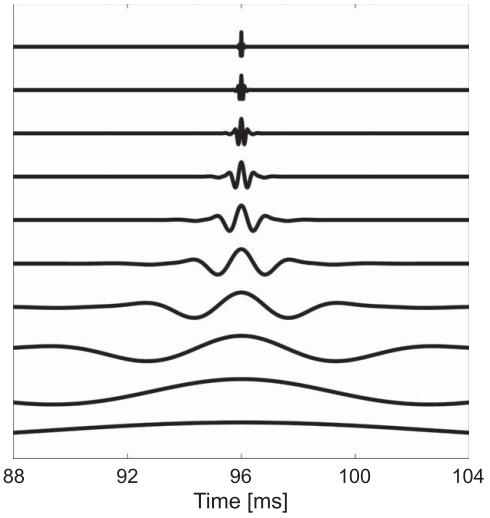

Fig. 9. Band filter impulse responses of the proposed GEQ, using the Kaiser window, from the highest band (top) to the lowest one (bottom).

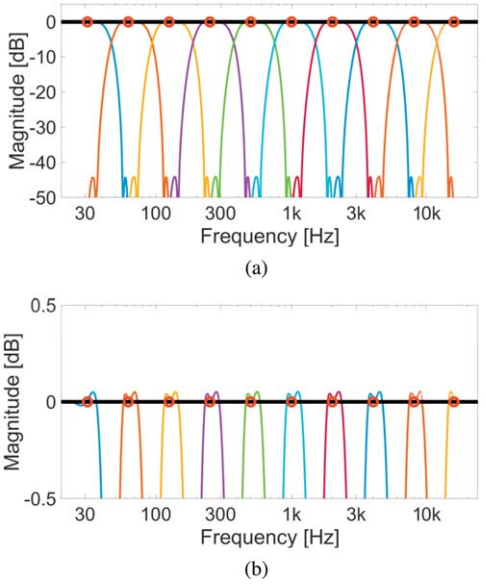

Fig. 10. (a) Magnitude responses of the band filters with all the command gains (circles) at 0 dB and (b) its details between −0.5 dB and 0.5 dB. The solid black line shows the total response.

(b) the special zigzag setting: [12 -12 -12 12 -12 -12 12 -12 -12 12] dB, which is declared the most difficult case for the equalizer of [47];

(c) an arbitrary setting [8 10 -9 10 3 -10 -6 1 11 12] dB.

In Fig. 11, the response obtained by applying the Blackman window with $N = 54$ and the one obtained with the Kaiser window with $N = 18$ are reported. Although the Blackman window with $N = 54$ guarantees the lowest error (0.05 dB), the final equalizer shows steeper transition bands. However, sharp transitions lead to a lengthening of the impulse response, and thus, more audible pre-ringing for linear-phase filters, which can ruin the important transients of musical instrument sounds.

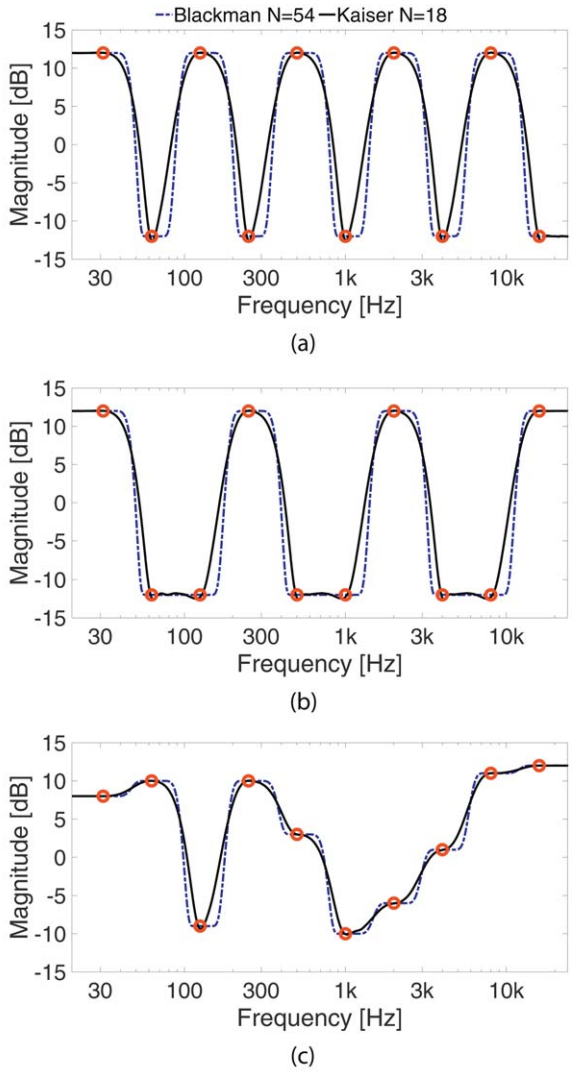

Fig. 11. Magnitude response of the proposed equalizer for two different prototype filters, considering (a) the zigzag configuration (±12 dB), (b) the gains [12 -12 -12 12 -12 -12 12 -12 -12 12] dB, and (c) the arbitrary gains [8 10 -9 10 3 -10 -6 1 11 12] dB.

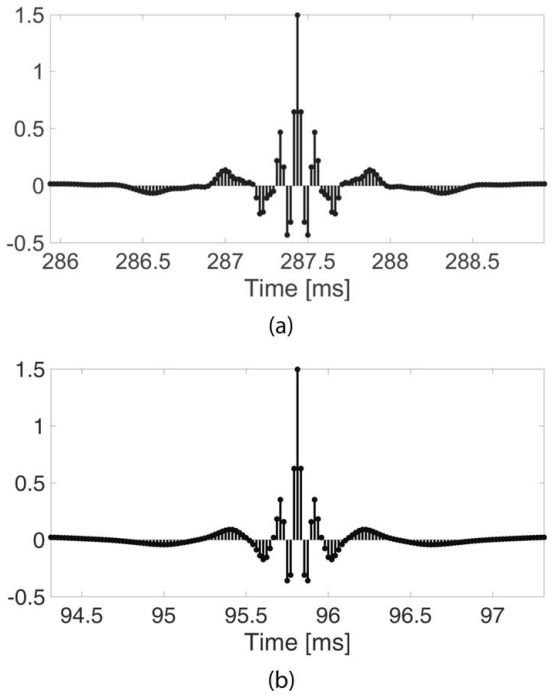

Fig. 12. Impulse response of the proposed equalizer designed using (a) the Blackman window with an order of $N = 54$ and (b) the Kaiser window with an order of $N = 18$ for the configuration of Fig. 11(a).

Fig. 12 shows total impulse responses of the proposed GEQ for the first configurations of Fig. 11 comparing the Blackman widow and the Kaiser window. All the impulse responses in Fig. 12 are symmetric, which also proves the linear-phase of each band filter and the total response of the equalizer.

The proposed system has been tested also varying the sampling frequency f_s. A sampling frequency of 44.1 kHz produces a slight decrease of the center frequencies with the ratio of $44.1/48 = 0.918$, but otherwise the same performance is obtained using the same filter coefficients. However, higher sampling rates, such as 88.2 kHz and 96 kHz, would require a larger prototype filter order N to guarantee an acceptable error.

2 COMPARISON WITH OTHER METHODS

Next, the proposed equalizer is compared with previous linear-phase FIR GEQ designs in terms of latency and computational cost. The FFT-based equalizer of Schöpp and Hetze [29] and a single FIR GEQ [20] obtained from the proposed structure are included in the comparison. Other linear-phase, multirate state-of-the-art approaches, such as the multirate GEQ of [32], have not been considered in the comparison, because they have a very large latency and computational cost, not competitive with the proposed method.

The FFT-based equalizer of [29] consists in the design of a target frequency response of the equalizer that depends on the desired gains and on the filtering of the input signal with that frequency response using the overlap and add method with an overlap of 50% [48]. Here, the target frequency response is calculated by summing the filter responses of the proposed IFIR structure. The FFT length of 16,384 is chosen to obtain the same response and the same error as the proposed implementation, so the frame size of the overlap and add method has a length of 8,192 samples.

The single FIR method, similarly to the FFT-based one, is formed as the sum of the filter responses of the proposed IFIR structure and executes the time-domain convolution. The length of the single FIR filter is 9,199, and it produces the same error as the proposed equalizer.

Table 3 compares the proposed equalizer and the other two methods in terms of latency and computational cost. For each method, the table shows the latency in samples of the total equalizer and the number of multiplications and additions per output sample. All three methods have exactly the same transfer function and thus, the same error equal to 0.79 dB, as shown in Table 2.

Table 3. Performance of the proposed equalizer (the Kaiser window design) compared with other linear-phase GEQs. The symmetry has been accounted for in the number of multiplications. The best result in each column is highlighted.

Method	Latency	Mul	Add
Single FIR	**4,599**	4,600	9,198
FFT	20,983	116	168
Proposed	**4,599**	**64**	**108**

The FFT-based and the single FIR methods use the same filters but apply different implementations. Table 3 shows that the FFT method presents the largest latency because of the frame-based FFT processing that introduces an algorithmic delay of 16,384 samples in addition to the filter group delay of 4,599 samples. The latency could be reduced using the zero-latency partitioned convolution [49, 50]. In that case, the latency would be the same as that of the proposed method but the computational cost would be larger. Table 3 also shows that the FFT GEQ needs considerably more multiplications and additions (284 operations, in total) than the proposed method (172 in total). The proposed method thus requires 39% fewer operations per sample than the FFT method.

The time-domain filtering carried out with the single FIR presents the same latency as the proposed method but 80 times larger computational complexity, which is seen by comparing the number of multiplications and additions in Table 3. The proposed method shows the best performance in terms of latency (4,599 samples or 95.8 ms, which is 78% less than the FFT method) and computational complexity (172 operations per sample, of which 64 multiplications and 108 additions).

The computational complexity of the proposed equalizer is competitive even with IIR filters. The state-of-the-art IIR octave GEQ uses 50 multiplications per sample [51], that is, 78% of the multiplications needed by the proposed GEQ (64 multiplications per sample). The required delay memory is much larger in the proposed method than in IIR equalizers, however. Additionally, the proposed GEQ does not require any operations when the command gains are changed, whereas in IIR-based GEQs, the filter gains must be optimized, e.g., using a neural network [52, 9].

The fairly large latency of the proposed method, almost 100 ms, seems large, but is acceptable in audio playback. It still raises a question whether this much latency could cause a synchronization problem when sound is associated with video. However, an ITU recommendation states that the detection threshold for latency of sound with respect to vision is 125 ms and the acceptability threshold is 185 ms [53]. This implies that the latency of the proposed method by itself does not exceed the detection threshold in audio-visual synchronization.

3 CONCLUSION

This paper presents a novel design of a linear-phase graphic equalizer with octave-band division. The design is based on IFIR filters, which use the concept of interpolation of filter responses but does not split the input signal into subbands. All band filters are based on a linear-phase low-pass prototype FIR filter, which is designed using the windowing method. The use of the proposed GEQ is effortless, as the command gains can be used as weights in the filter structure without optimization. The performance of the proposed equalizer has been evaluated considering different window functions in the prototype filter design. The best performance is obtained using the Kaiser window.

The proposed graphic equalizer has been compared with other existing linear-phase graphic equalizers in terms of computational load and latency. The proposed method guarantees the lowest computational cost, which is smaller than that of the FFT-based implementation and only slightly larger than that of a state-of-the-art IIR GEQ. The proposed design offers the lowest latency among the tested linear-phase techniques, which is less than 100 ms. The proposed method also has a maximum frequency-response error smaller than 1 dB among all the possible command settings with $\pm$12-dB gains. Therefore, the experimental results prove the effectiveness of the proposed linear-phase structure based on IFIR filters. The linear-phase GEQ is useful in audio applications in which it is important not to distort the phase of the signal, such as in stereo and multichannel equalization.

4 ACKNOWLEDGMENT

This work was conducted in September–December 2021, when the first author was a visiting researcher at the Aalto Acoustics Lab, Espoo, Finland. This research is part of the activities of the Nordic Sound and Music Computing Network—NordicSMC (NordForsk project no. 86892).

5 REFERENCES

[1] R. A. Greiner and M. Schoessow, "Design Aspects of Graphic Equalizers," *J. Audio Eng. Soc.*, vol. 31, no. 6, pp. 394–407 (1983 Jun.).

[2] S. K. Mitra and J. F. Kaiser, *Handbook for Digital Signal Processing* (John Wiley & Sons, New York, USA, 1993), 1st ed.

[3] V. Välimäki and J. D. Reiss, "All About Audio Equalization: Solutions and Frontiers," *Appl. Sci.*, vol. 6, no. 5, paper 129 (2016 May). https://doi.org/10.3390/app6050129.

[4] J. Vilkamo, T. Bäckström, and A. Kuntz, "Optimized Covariance Domain Framework for Time–Frequency Processing of Spatial Audio," *J. Audio Eng. Soc.*, vol. 61, no. 6, pp. 403–411 (2013 Jun.).

[5] A. Favrot and C. Faller, "Wiener-Based Spatial B-Format Equalization," *J. Audio Eng. Soc.*, vol. 68, nos. 7/8, pp. 488–494 (2020 Jul.).

[6] B. Radlovic and R. Kennedy, "Nonminimum-Phase Equalization and Its Subjective Importance in Room Acoustics," *IEEE Trans. Speech Audio Process.*, vol. 8, no. 6, pp. 728–737 (2000 Nov.). https://doi.org/10.1109/89.876311.

[7] Y. Hirata, "Digitalization of Conventional Analog Filters for Recording Use," *J. Audio Eng. Soc.*, vol. 29, no. 5, pp. 333–337 (1981 May).

[8] S. Prince and K. R. Shankar Kumar, "A Novel *N*th-order IIR Filter-Based Graphic Equalizer Optimized through Genetic Algorithm for Computing Filter Order," *Soft Comput.*, vol. 23, no. 8, pp. 2683–2691 (2019 Apr.). https://doi.org/10.1007/s00500-018-3640-9.

[9] J. Rämö, J. Liski, and V. Välimäki, "Third-Octave and Bark Graphic-Equalizer Design with Symmetric Band Filters," *Appl. Sci.*, vol. 10, no. 4, paper 1222 (2020 Feb.). https://doi.org/10.3390/app10041222.

[10] S. Tassart, "Graphical Equalization Using Interpolated Filter Banks," *J. Audio Eng. Soc.*, vol. 61, no. 5, pp. 263–279 (2013 May).

[11] J. Rämö, V. Välimäki, and B. Bank, "High-Precision Parallel Graphic Equalizer," *IEEE/ACM Trans. Audio Speech Lang. Process.*, vol. 22, no. 12, pp. 1894–1904 (2014 Dec.). https://doi.org/10.1109/TASLP.2014.2354241.

[12] J. Liski, B. Bank, J. O. Smith, and V. Välimäki, "Converting Series Biquad Filters into Delayed Parallel Form: Application to Graphic Equalizers," *IEEE Trans. Signal Process.*, vol. 67, no. 14, pp. 3785–3795 (2019 Jul.). https://doi.org/10.1109/TSP.2019.2919419.

[13] D. A. Bohn, "Constant-Q Graphic Equalizers," *J. Audio Eng. Soc.*, vol. 34, no. 9, pp. 611–626 (1986 Sep.).

[14] V. Välimäki and J. Liski, "Accurate Cascade Graphic Equalizer," *IEEE Signal Process. Lett.*, vol. 24, no. 2, pp. 176–180 (2017 Feb.). https://doi.org/10.1109/LSP.2016.2645280.

[15] N. Agrawal, A. R. Kumar, and V. Bajaj, "A New Design Method for Stable IIR Filters with Nearly Linear-Phase Response Based on Fractional Derivative and Swarm Intelligence," *IEEE Trans. Emerg. Top. Comput. Intell.*, vol. 1, no. 6, pp. 464–477 (2017 Dec.). https://doi.org/10.1109/TETCI.2017.2748151.

[16] K. Horváth and B. Bank, "Optimizing the Numerical Noise of Parallel Second-Order Filters in Fixed-Point Arithmetic," *J. Audio Eng. Soc.*, vol. 67, no. 10, pp. 763–771 (2019 Oct.). https://doi.org/10.17743/jaes.2019.0027.

[17] J. A. Jensen, "A New Principle for an All-Digital Preamplifier and Equalizer," *J. Audio Eng. Soc.*, vol. 35, no. 12, pp. 994–1003 (1987 Dec.).

[18] J. Henriquez, T. Riemer, and R.Jr Trahan, "A Phase-Linear Audio Equalizer: Design and Implementation," *J. Audio Eng. Soc.*, vol. 38, no. 9, pp. 653–666 (1990 Sept.).

[19] M. Waters, M. Sandler, and A. C. Davies, "Low-Order FIR Filters for Audio Equalization," presented at the *91st Convention of the Audio Engineering Society* (1991 Oct.), paper 3188.

[20] D. S. McGrath, "An Efficient 30-Band Graphic Equalizer Implementation for a Low-Cost DSP Processor," presented at the *95th Convention of the Audio Engineering Society* (1993 Oct.), paper 3756.

[21] P. H. Kraght, "A Linear-Phase Digital Equalizer with Cubic-Spline Frequency Response," *J. Audio Eng. Soc.*, vol. 40, no. 5, pp. 403–414 (1992 May).

[22] D. S. McGrath, "A New Approach to Digital Audio Equalization," presented at the *97th Convention of the Audio Engineering Society* (1994 Nov.), paper 3899.

[23] R. Väänänen and J. Hiipakka, "Efficient Audio Equalization Using Multirate Processing," *J. Audio Eng. Soc.*, vol. 56, no. 4, pp. 255–266 (2008 Apr.).

[24] M. K. Othman and T. H. Lim, "Run Time Analysis of an Audio Graphic Equalizer for Portable Industrial Directional Sound Systems in Industrial Usage," in *Proceedings of the 14th IEEE Conference on Industrial Electronics and Applications (ICIEA)*, pp. 2177–2181 (Xi'an, China) (2019 Jun.). https://doi.org/10.1109/ICIEA.2019.8833760.

[25] R. J. Oliver, "Frequency-Warped Audio Equalizer," US Patent 7,764,802 B2 (2010 Jul.).

[26] J. Siiskonen, *Graphic Equalization Using Frequency-Warped Digital Filters*, Master's thesis, Aalto University School of Electrical Engineering, Espoo, Finland (2016 Jul.).

[27] T. G.Jr. Stockham, "High-Speed Convolution and Correlation," in *Proceedings of the Spring Joint Computer Conference*, vol. 28, pp. 229–233 (New York, USA) (1966 Apr.).

[28] B. D. Kulp, "Digital Equalization Using Fourier Transform Techniques," presented at the *85th Convention of the Audio Engineering Society* (1988 Nov.), paper 2694.

[29] H. Schöpp and H. Hetze, "A Linear-Phase 512-Band Graphic Equalizer using the Fast-Fourier Transform," presented at the *96th Convention of the Audio Engineering Society* (1994 Feb.), paper 3816.

[30] G. F. P. Fernandes, L. G. P. M. Martins, M. F. M. Sousa, F. S. Pinto, and A. J. S. Ferreira, "Implementation of a New Method to Digital Audio Equalization," presented at the *106th Convention of the Audio Engineering Society* (1999 May), paper 4895.

[31] S. Ries and G. Frieling, "PC-Based Equalizer with Variable Gain and Delay in 31 Frequency Bands," presented at the *108th Convention of the Audio Engineering Society* (2000 Feb.), paper 5173.

[32] S. Cecchi, L. Palestini, E. Moretti, and F. Piazza, "A New Approach to Digital Audio Equalization," in *Proceedings of the IEEE Workshop on Applications of Signal Processing to Audio and Acoustics (WASPAA)*, pp. 62–65 (New Paltz, NY, USA) (2007 Oct.). https://doi.org/10.1109/ASPAA.2007.4393011.

[33] R. Hergum, "A Low Complexity, Linear Phase Graphic Equalizer," presented at the *85th Convention of the Audio Engineering Society* (1988 Nov.), paper 2738.

[34] Y. Neuvo, D. Cheng-Yu, and S. Mitra, "Interpolated Finite Impulse Response Filters," *IEEE Trans. Acoust. Speech Signal Process.*, vol. 32, no. 3, pp. 563–570 (1984 Jun.), https://doi.org/10.1109/TASSP.1984.1164348.

[35] V. Bruschi, S. Nobili, A. Terenzi, and S. Cecchi, "A Low-Complexity Linear-Phase Graphic Audio Equalizer Based on IFIR Filters," *IEEE Signal Process. Lett.*, vol. 28, pp. 429–433 (2021 Feb.). https://doi.org/10.1109/LSP.2021.3057228.

[36] M. Holschneider, R. Kronland-Martinet, J. Morlet, and P. Tchamitchian, "A Real-Time Algorithm

for Signal Analysis with the Help of the Wavelet Transform," in J. M. Combes, A. Grossmann, and P. Tchamitchian (Eds.), *Wavelets, Time-Frequency Methods and Phase Space*, Inverse Problems and Theoretical Imaging, pp. 286–297 (Springer, Berlin/Heidelberg, Germany, 1989). https://doi.org/10.1007/978-3-642-75988-8_28.

[37] P. P. Vaidyanathan, "Multistage Implementations," in *Multirate Systems and Filterbanks*, pp. 134–143 (Prentice-Hall, Inc., Upper Saddle River, NJ, USA, 1993).

[38] J. Rämö, V. Välimäki, and M. Tikander, "Perceptual Headphone Equalization for Mitigation of Ambient Noise," in *Proceedings of the IEEE International Conference on Acoustics, Speech and Signal Processing (ICASSP)*, pp. 724–728 (Vancouver, Canada) (2013 May).

[39] A. V. Oppenheim and R. W. Schafer, "Filter Design Techniques," in *Discrete-Time Signal Processing*, pp. 439–511 (Prentice-Hall, Inc., Upper Saddle River, NJ, 1999).

[40] E. Wesfreid and M. Wickerhauser, "Adapted Local Trigonometric Transforms and Speech Processing," *IEEE Trans. Signal Process.*, vol. 41, no. 12, pp. 3596–3600 (1993 Dec.), https://doi.org/10.1109/78.258104.

[41] J. F. Kaiser, "Nonrecursive Digital Filter Design Using the I_0-sinh Window Function," in *Proceedings of the IEEE International Symposium on Circuits & Systems (ISCAS)*, pp. 20–23 (San Francisco, CA) (1974 Apr.).

[42] J. Liski and V. Välimäki, "The Quest for the Best Graphic Equalizer," in *Proceedings of the 20th International Conference on Digital Audio Effects (DAFx)*, pp. 95–102 (Edinburgh, UK) (2017 Sep.).

[43] M. Holters and U. Zölzer, "Graphic Equalizer Design Using Higher-Order Recursive Filters," in *Proceedings of the International Conference on Digital Audio Effects (DAFx)*, pp. 37–40 (Montreal, Canada) (2006 Sep.).

[44] F. E. Toole and S. E. Olive, "The Modification of Timbre by Resonances: Perception and Measurement," *J. Audio Eng. Soc.*, vol. 36, no. 3, pp. 122–142 (1988 Mar.).

[45] L. D. Fielder, "Analysis of Traditional and Reverberation-Reducing Methods of Room Equalization," *J. Audio Eng. Soc.*, vol. 51, nos. 1/2, pp. 3–26 (2003 Feb.).

[46] H. Korhola and M. Karjalainen, "Perceptual Study and Auditory Analysis on Digital Crossover Filters," *J. Audio Eng. Soc.*, vol. 57, no. 6, pp. 413–429 (2009 Jun.).

[47] R. J. Oliver and J.-M. Jot, "Efficient Multi-band Digital Audio Graphic Equalizer with Accurate Frequency Response Control," presented at the *139th Convention of the Audio Engineering Society* (2015 Oct.), paper 9406.

[48] J. J. Shynk, "Frequency-Domain and Multirate Adaptive Filtering," *IEEE Signal Process. Mag.*, vol. 9, no. 1, pp. 14–37 (1992 Jan.). https://doi.org/10.1109/79.109205.

[49] W. G. Gardner, "Efficient Convolution Without Input/Output Delay," *J. Audio Eng. Soc.*, vol. 43, no. 3, pp. 127–136 (1995 Mar.).

[50] F. Wefers and J. Berg, "High-Performance Real-Time FIR-Filtering using Fast Convolution on Graphics Hardware," in *Proceedings of the 13th International Conference on Digital Audio Effects (DAFx)* (Graz, Austria) (2010 Sep.).

[51] J. Liski, J. Rämö, and V. Välimäki, "Graphic Equalizer Design with Symmetric Biquad Filters," in *Proceedings of the IEEE Workshop on Applications of Signal Processing to Audio and Acoustics (WASPAA)*, pp. 55–59 (New Paltz, NY, USA) (2019 Oct.).

[52] V. Välimäki and J. Rämö, "Neurally Controlled Graphic Equalizer," *IEEE/ACM Trans. Audio Speech Lang. Process.*, vol. 27, no. 12, pp. 2140–2149 (2019 Dec.). https://doi.org/10.1109/TASLP.2019.2935809.

[53] International Telecommunication Union, "Relative Timing of Sound and Vision for Broadcasting," *Recommendation ITU-R BT.1359-1* (1998 Nov.).

THE AUTHORS


Valeria Bruschi


Vesa Välimäki


Juho Liski


Stefania Cecchi

Valeria Bruschi was born in Ancona, Italy, in 1994. In 2018, she received an M.Sc. degree in electronic engineering from Università Politecnica delle Marche, Ancona, Italy. She is currently a Ph.D. student at the Department of Information Engineering at Università Politecnica delle Marche. Her research interests are mainly focused on digital audio signal processing applied on audio equalization and immersive audio systems. She is a Student Member of the Audio Engineering Society (AES).

•

Vesa Välimäki is the Professor of Audio Signal Processing and Vice Dean for Research at Aalto University, Espoo, Finland. He received his M.Sc. and D.Sc. degrees from the Helsinki University of Technology in 1992 and 1995, respectively. In 2008–2009, he was a visiting scholar at the Stanford University Center for Computer Research in Music and Acoustics (CCRMA). His research interests are in signal processing and machine learning applied to audio and music technology. He is a Fellow of the AES and a Fellow of the Institute of Electrical and Electronics Engineers (IEEE). Prof. Välimäki is the Editor-in-Chief of the Journal of the AES.

•

Juho Liski was born in Helsinki, Finland, in 1989. He received an M.Sc. and a Doctor of Science in Technology degree in electrical engineering from the Aalto University School of Electrical Engineering, Espoo, Finland, in 2016 and 2020, respectively. He has been working at the Acoustics Lab of the Aalto University School of Electrical Engineering since 2015 and is currently a postdoctoral researcher, focusing on audio signal processing and equalization. Dr. Liski is a Member of the Acoustical Society of Finland.

•

Stefania Cecchi was born in Amandola, Italy, in 1979. She received a Laurea degree (with honors) in electronic engineering from the University of Ancona (now University Politecnica delle Marche, Italy) in 2004 and a Ph.D. degree in electronic engineering from the University Politecnica delle Marche (Ancona, Italy) in 2007. She was a postdoc researcher at DII (Department of Information Engineering) at the same university from February 2008 to October 2015 and an Assistant Professor from November 2015 to October 2018. She is an Associate Professor at the same department since November 2018. She is the author or coauthor of numerous international papers. Her current research interests are in the area of digital signal processing, including adaptive DSP algorithms and circuits, speech, and audio processing. Prof. Cecchi is a member of the AES, IEEE, and the Italian Acoustical Association (AIA).